SMALL-SIZE PRINTED MONOPOLE WITH A PRINTED DISTRIBUTED INDUCTOR FOR PENTABAND WWAN MOBILE PHONE APPLICATION

Chih-Hua Chang and Kin-Lu Wong
Department of Electrical Engineering, National Sun Yat-Sen University, Kaohsiung 80424, Taiwan, People's Republic of China; Corresponding author: changch@ema.ee.nsysu.edu.tw

Received 15 March 2009

ABSTRACT: *In this article, a small-size printed monopole embedded with a printed narrow strip as a distributed inductor for application in the mobile phone to achieve GSM850/900/1800/1900/UMTS pentaband wireless wide area network operation is presented. With the printed distributed inductor, the fundamental (lowest) resonant mode of the proposed antenna can be effectively shifted to lower frequencies with a wide operating bandwidth, owing to the contributed inductance of the printed distributed inductor compensating for the increased capacitance resulting from the decreased resonant length of the monopole. In this study, the proposed antenna can be printed on the small no-ground portion of size 14 × 40 mm^2 on the main circuit board of the mobile phone, making it easy to fabricate at low cost and generally showing no thickness above the circuit board; the latter is very attractive for thin-profile mobile phone applications. The proposed monopole antenna is studied in detail in this article. The results also show that the antenna is very suitable to be placed at the bottom of the mobile phone; in this case, the antenna meets the specific absorption rate limit for practical applications.* © 2009 Wiley Periodicals, Inc. Microwave Opt Technol Lett 51: 2903–2908, 2009; Published online in Wiley InterScience (www.interscience.wiley.com). DOI 10.1002/mop.24775

Key words: *mobile antennas; handset antennas; WWAN antennas; multiband antennas; internal mobile phone antennas*

1. INTRODUCTION

The chip-inductor-embedded small-size printed monopole for wireless wide area network (WWAN) operation in the mobile phone has recently been demonstrated [1]. The printed monopole occupies a small area of 15 × 34 mm^2 on the no-ground portion of the main circuit board of the mobile phone and generally shows no thickness above the circuit board, which is very attractive for thin-profile mobile phone or laptop computer applications [2–15]. The much reduced size of the chip-inductor-embedded monopole is mainly owing to the additional inductance contributed by the chip inductor to compensate for the increased capacitance resulting from the decreased resonant length of the monopole [16, 17]. However, with the lumped chip inductor, additional process in the fabrication of the antenna is required, which increases the fabrication cost.

In this article, we present a printed monopole embedded with a printed narrow strip as a distributed inductor for application in the mobile phone to achieve GSM850/900/1800/1900/UMTS pentaband WWAN operation. The printed distributed inductor replaces the lumped chip inductor, leading to an all-printed structure for the proposed small-size monopole applied as an internal WWAN mobile phone antenna. The proposed printed monopole, hence, can be implemented at low cost. In addition, it has a similar small size as that in [1] for the case of using a lumped chip inductor and can be printed on a no-ground portion of 14 × 40 mm^2 on the main circuit board of the mobile phone (Fig. 1). Further, the use of a distributed inductor can decrease the possible losses associated with the use of a lumped chip inductor (such as the conductive loss associated with the bending and winding of the strips in the chip inductor and the dielectric loss in the chip element) [18]. Detailed effects of the printed distributed inductor on the proposed small-size monopole are studied in this article. The specific absorption rate (SAR) [19–22] results of the proposed antenna placed at the bottom of the mobile phone are also shown. The results indicate that the obtained SAR values meet the limit of 1.6 W/kg for the 1-g head tissue and 2.0 W/kg for the 10-g head tissue [19]. Details of the results are presented and discussed.

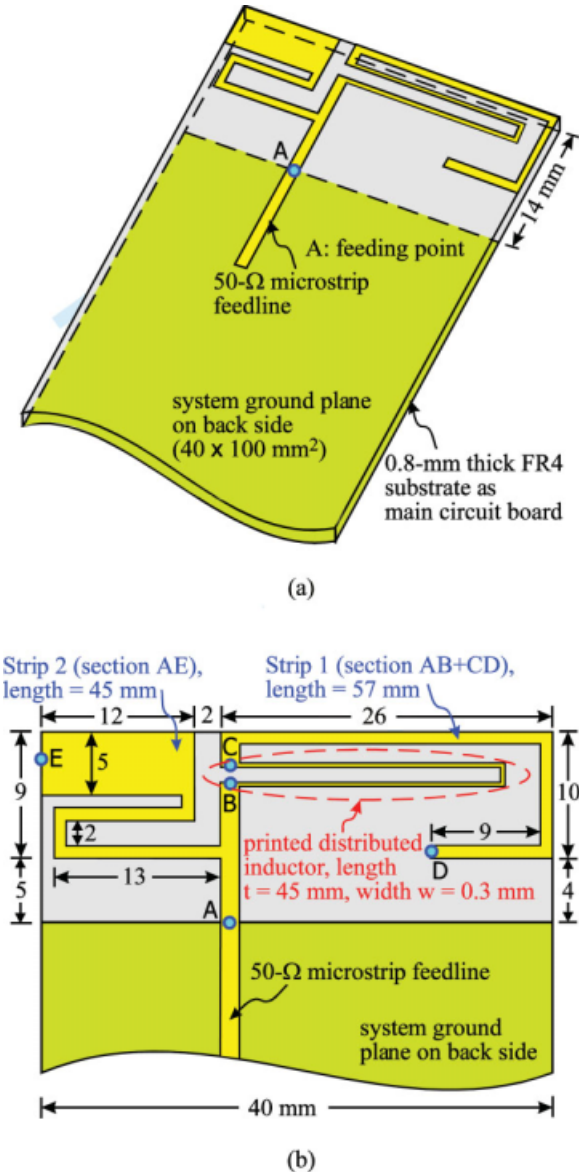

Figure 1 (a) Geometry of the proposed small-size printed monopole with a printed distributed inductor for pentaband WWAN operation in the mobile phone. (b) Dimensions of the proposed antenna. [Color figure can be viewed in the online issue, which is available at www.interscience.wiley.com]

2. PROPOSED ANTENNA

Figure 1(a) shows the geometry of the proposed small-size printed monopole with a printed distributed inductor for pentaband WWAN operation in the mobile phone. The proposed monopole is printed on the no-ground portion of size 14 × 40 mm^2 on the main circuit board of the mobile phone. A

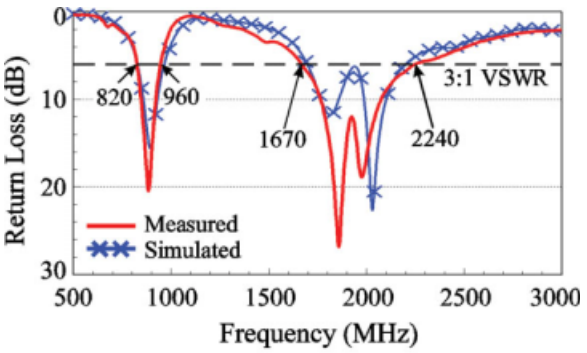

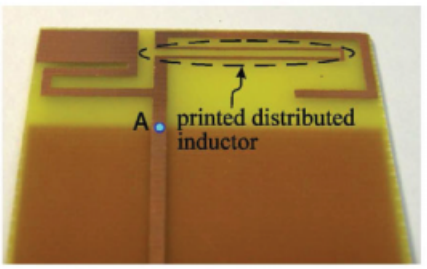

Figure 2 (a) Measured and simulated (HFSS) return loss for the fabricated antenna. (b) Photo of the antenna. [Color figure can be viewed in the online issue, which is available at www.interscience.wiley.com]

0.8-mm-thick FR4 substrate is used as the main circuit board in the study, and the system ground plane of size 100×40 mm^2 is printed on the back side of the circuit board. The proposed printed monopole is a two-strip monopole whose dimensions are given in Figure 1(b). Strip 1 is the longer strip and has a length of 57 mm (section AB and CD in the figure). In-between point B and C, a narrow strip (width $w = 0.3$ mm) of length 45 mm (t) is printed, which functions as a distributed inductor with an equivalent inductance of about 15 nH (see the results presented in Fig. 4 and will be discussed in the next section).

With this distributed inductor, strip 1 can resonate at about 900 MHz, although it has a length of 57 mm only or about 0.17λ at 900 MHz (excluding the length of the distributed inductor), resulting in a wide lower band for the antenna to cover GSM850 (824–894 MHz) and GSM900 (880–960 MHz) operation. In addition, because of the presence of the printed distributed inductor, a higher-order mode at about 2000 MHz contributed by strip 1 can also be generated. This higher-order mode incorporates the resonant mode excited at about 1800 MHz contributed by strip 2 of length 45 mm or about 0.27λ at 1800 MHz (the shorter strip, section AE in the figure) to form a wide upper band for the antenna to cover GSM1800 (1710–1880 MHz), GSM1900 (1850–1990 MHz), and UMTS (1920–2170 MHz) operation. Hence, with the distributed-inductor-loaded strip 1 and the simple strip 2 for the proposed antenna, two wide operating bands for covering GSM850/900/1800/1900/UMTS pentaband WWAN operation are obtained. For testing the proposed antenna in the experiment, a 50-Ω microstrip feedline printed on the front side of the circuit board is connected to point A (the antenna's feeding point), and effects of the distributed inductor on the antenna performances are analyzed.

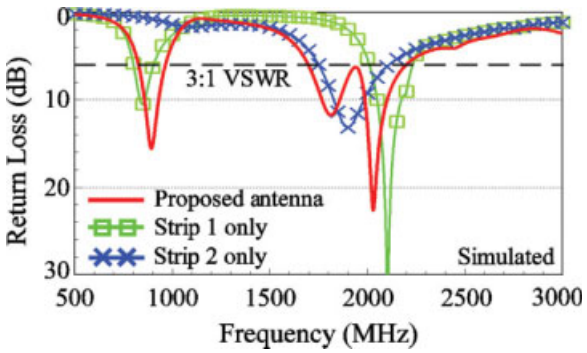

Figure 3 Simulated (HFSS) return loss for the proposed antenna, the case with strip 1 only and the case with strip 2 only. [Color figure can be viewed in the online issue, which is available at www.interscience.wiley.com]

3. RESULTS AND DISCUSSION

The proposed antenna was fabricated and studied. Figure 2(a) presents the measured and simulated return loss, and the photo of the fabricated antenna is also shown in Figure 2(b). Agreement between the measured data and the simulated results obtained using Ansoft HFSS [23] is seen. Two wide operating bands at about 900 and 1900 MHz are obtained. With the definition of 3:1 VSWR (6-dB return loss) generally used for the internal mobile phone antenna design, the lower band covers GSM850/900 operation, while the upper band formed by two resonant modes covers GSM1800/1900/UMTS operation; the results agree with the discussion given in Section 2.

To analyze the effects of strip 1 and strip 2 on the antenna performance, Figure 3 shows the simulated return loss for the proposed antenna, the case with strip 1 only and the case with strip 2 only. The results clearly show that strip 2 contributes a resonant mode at about 1800 MHz, whereas strip 1 generates two resonant modes with one at about 900 MHz and the second

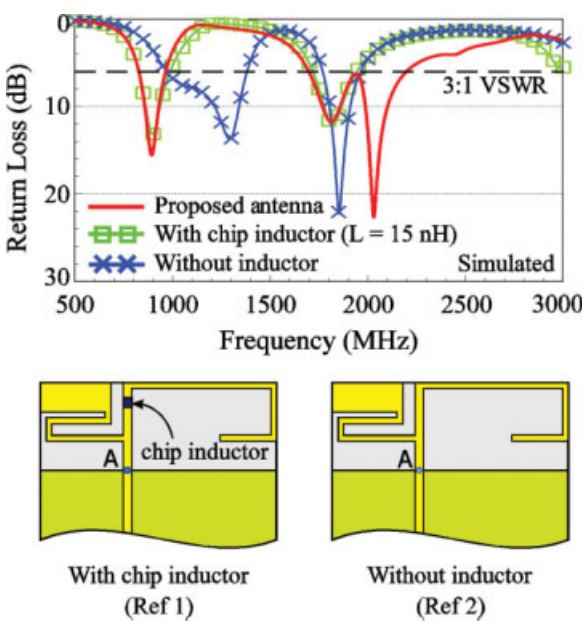

Figure 4 Simulated (HFSS) return loss for the proposed antenna, the case with a chip inductor of 15 nH replacing the printed distributed inductor (Ref. 1) and the case without the printed distributed inductor or chip inductor (Ref. 2). [Color figure can be viewed in the online issue, which is available at www.interscience.wiley.com]

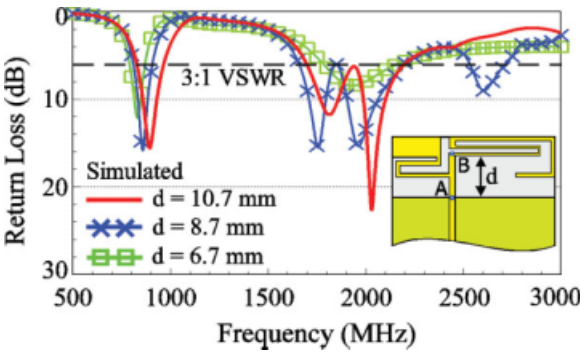

Figure 5 Simulated (HFSS) return loss for the proposed antenna as a function of the position d of the printed distributed inductor. Other dimensions are the same as given in Figure 1. [Color figure can be viewed in the online issue, which is available at www.interscience.wiley.com]

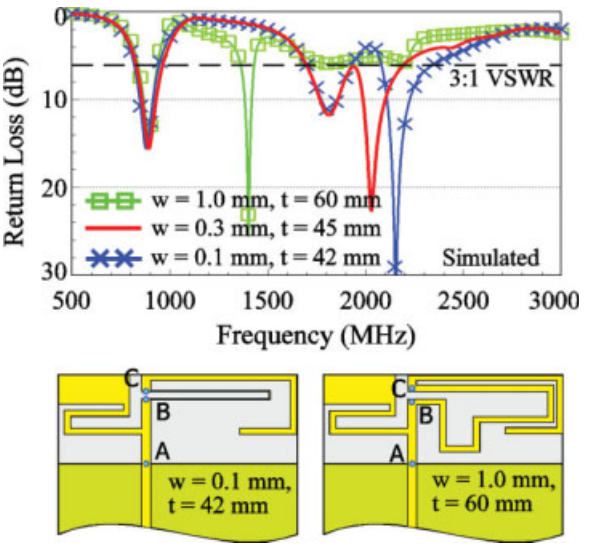

Figure 6 Simulated (HFSS) return loss for different dimensions of the printed distributed inductor to achieve the resonant mode at about 900 MHz. Other dimensions are the same as given in Figure 1. [Color figure can be viewed in the online issue, which is available at www.interscience.wiley.com]

one at about 2000 MHz. The loading effects of the printed distributed inductor are further analyzed in Figure 4, in which results for the simulated return loss for the proposed antenna, the case with a chip inductor of 15 nH replacing the printed distributed inductor (Ref. 1), and the case without the printed distributed inductor or chip inductor (Ref. 2) are shown. For both the proposed antenna and Ref. 1, a resonant mode at about 900 MHz is generated, while the lowest resonant mode for Ref. 2 is centered at about 1200 MHz only. This suggests that the printed distributed inductor used in the proposed antenna has an equivalent inductance of 15 nH and the additional inductance can indeed result in the decrease of the antenna's lowest resonant mode. Furthermore, from the comparison of the proposed antenna and Ref. 1, there is an additional resonant mode generated at about 2000 MHz, which is owing to the use of the printed distributed inductor instead of the chip inductor.

Figure 5 shows the simulated return loss for the proposed antenna as a function of the position d of the printed distributed inductor. The results for d varied from 6.7 to 10.7 mm are shown. Strong effects of the position d on the antenna's lower and upper bands are seen. The results indicate that the printed distributed inductor should not be too close to the connecting point of strip 1 and strip 2. For the case of $d = 10.7$ mm used in the proposed antenna (distributed inductor away from the connecting point of the two strips), good excitation of both strip 1 and strip 2 to achieve wide operating bandwidths can be obtained.

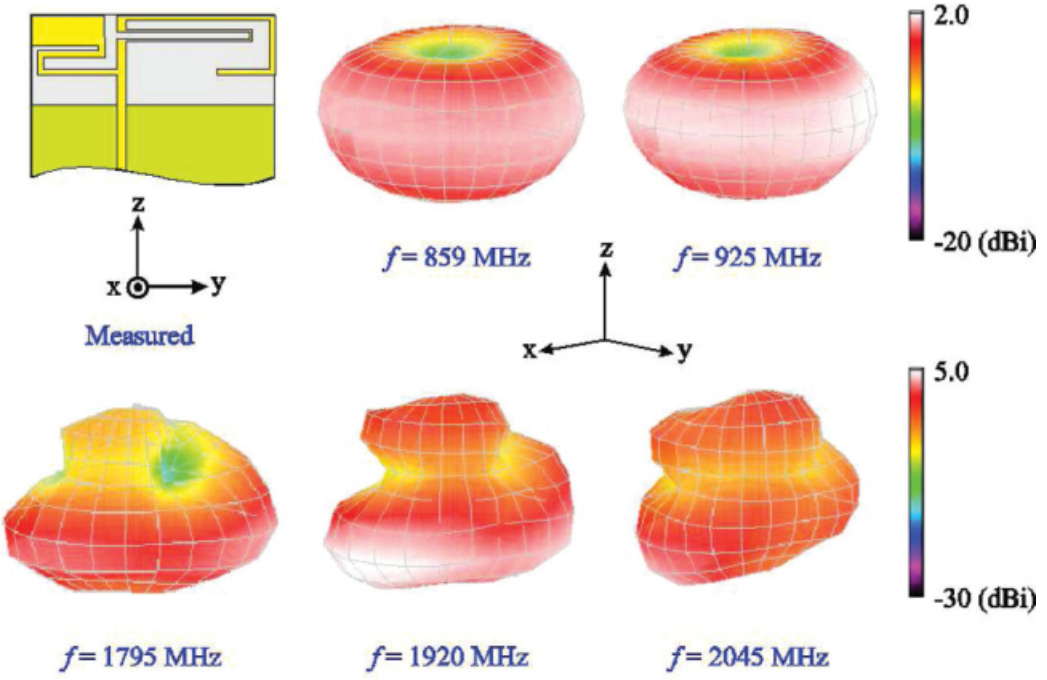

Figure 7 Measured 3-D radiation patterns for the proposed antenna. [Color figure can be viewed in the online issue, which is available at www.interscience.wiley.com]

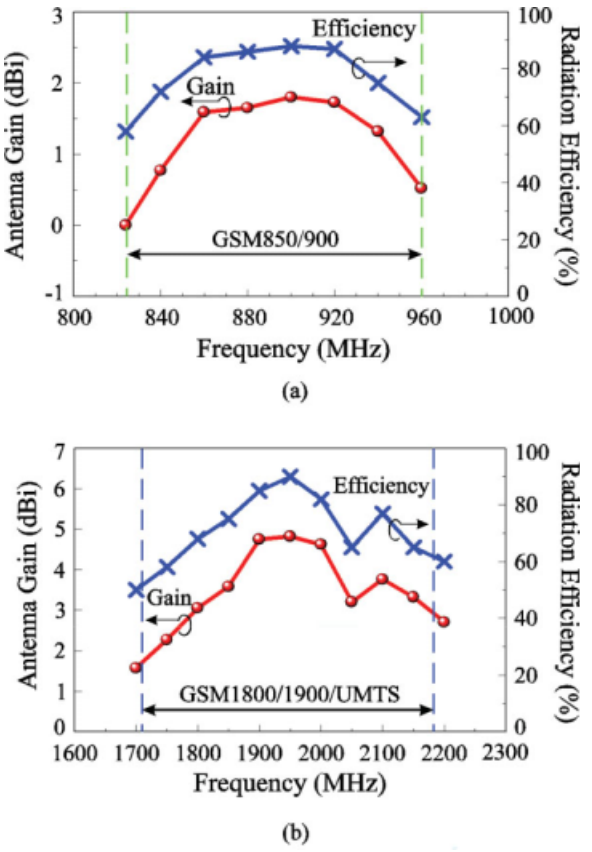

Figure 8 Measured radiation efficiency and antenna gain for the proposed antenna. (a) GSM850/900 bands. (b) GSM1800/1900/UMTS bands. [Color figure can be viewed in the online issue, which is available at www.interscience.wiley.com]

The dimensions (length and width) of the printed distributed inductor to achieve the desired resonant mode at about 900 MHz are also studied in Figure 6. The results of the simulated return loss for three different dimensions are presented. The case of $w = 0.3$ mm and $t = 45$ mm is used in the proposed antenna. When a smaller width ($w = 0.1$ mm) is selected, a shorter length ($t = 42$ mm) of the distributed inductor can be used. When the width w is widened to 1.0 mm, the required length t should be increased to 60 mm to provide sufficient inductance to compensate for the increased capacitance resulting from the decreased resonant length of strip 1 to resonate at about 900 MHz. Also note that when the width w is varied, the impedance matching for frequencies over the antenna's upper band is affected. Hence, there exists a proper width w for achieving good impedance matching for both the lower and upper bands. In this study, the case with the width $w = 0.3$ mm is selected for its good effects on the impedance matching of both the two operating bands of the antenna.

The radiation characteristics are also studied. Figure 7 shows the measured three-dimensional (3D) radiation patterns for the proposed antenna. Dipole-like radiation patterns at 859 and 925 MHz are seen, while more variations in the radiation patterns are observed at 1795, 1920, and 2045 MHz. The measured radiation patterns show no special distinctions when compared with those of the chip-inductor-embedded printed monopole for WWAN operation studied in [1] and many other internal WWAN mobile phone antennas that have been reported [24]. Figure 8 shows the measured radiation efficiency and antenna gain for the proposed antenna. For the frequencies

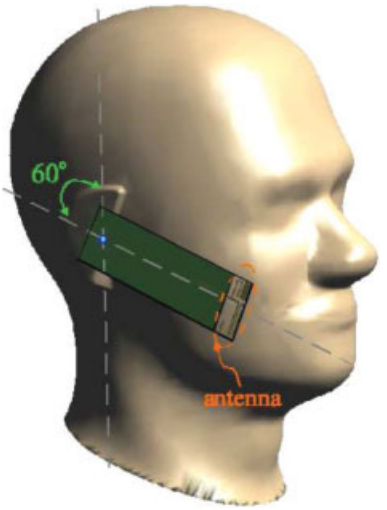

Figure 9 SAR simulation model (SEMCAD) for the proposed antenna. [Color figure can be viewed in the online issue, which is available at www.interscience.wiley.com]

over the GSM850/900 bands shown in Figure 8(a), the radiation efficiency is about 57–87%, and the antenna gain is about 0–1.7 dBi. Over the GSM1800/1900/UMTS bands in Figure 8(b), the radiation efficiency ranges from 50 to 89%, and the antenna gain varies from 1.6 to 4.8 dBi. The obtained radiation characteristics are acceptable for practical mobile phone applications.

The SAR results of the proposed antenna are also studied, and Figure 9 shows the SAR simulation model provided by SPEAG SEMCAD [25] in the study. Notice that the antenna is placed at the bottom of the mobile phone, which is a useful design that has been applied in some mobile phones for achieving decreased SAR of the internal mobile phone antenna [1, 20–22]. Table 1 lists the simulated SAR values for the 1-g and 10-g head tissues obtained using SEMCAD. The testing power in the SAR study is 24 dBm at lower frequencies (859 and 925 MHz) and 21 dBm at higher frequencies (1795, 1920, and 2045 MHz) [20]. For both cases, the SAR values are less than 1.6 W/kg (1-g head tissue) or 2.0 W/kg (10-g head tissue) [19], making the antenna very promising for practical mobile phone applications. The corresponding simulated SAR distributions (1-g head tissue) on the phantom head for the proposed antenna are also shown in Figure 10. On the phantom head, there is only one local SAR maximum for the lower frequencies (859 and 925 MHz), while there are two local SAR maxima for the higher frequencies (1795, 1920, and 2045 MHz). Since more local SAR maxima will lead to more smooth SAR distributions

TABLE 1 Simulated SAR in 1-g and 10-g Head Tissues Obtained from SEMCAD [25] for the Antenna Placed at the Bottom of the Mobile Phone with the Presence of the Phantom Head

Frequency (MHz)	SAR_{1g} (W/kg)	SAR_{10g} (W/kg)
859	1.53	1.09
925	1.37	0.96
1795	1.11	0.63
1920	0.57	0.32
2045	0.8	0.44

The top edge of the main circuit board is spaced 5 mm away from the phantom ear.

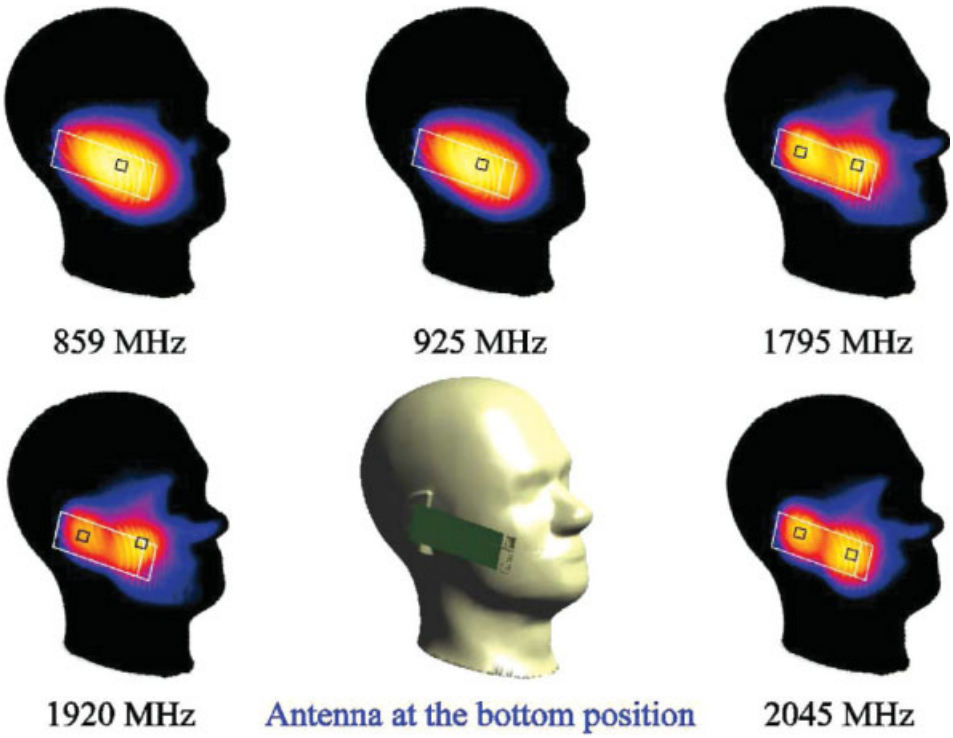

Figure 10 Simulated SAR distributions (1-g head tissue) on the phantom head for the proposed antenna. The open square marks indicate the local SAR maximum on the phantom head. [Color figure can be viewed in the online issue, which is available at www.interscience.wiley.com]

on the phantom head, it explains the observation of the decreased SAR values over the lower band than those over the upper band.

4. CONCLUSIONS

In this article, a small-size printed monopole consisting of a distributed-inductor-loaded longer strip and a simple shorter strip for achieving pentaband WWAN operation in the mobile phone has been proposed. The proposed antenna shows an all-printed uniplanar structure occupying a size of 14×40 mm^2 only, making it easy to fabricate at low cost for practical applications. The printed distributed inductor in the longer strip of the antenna shows an equivalent inductance of 15 nH, providing additional inductance to compensate for the increased capacitance resulting from the decreased resonant length of the longer strip for the 900 MHz band covering GSM850/900 operation. In addition, the distributed inductor studied here provides an additional higher-order mode to effectively widen the antenna's upper band to cover GSM1800/1900/UMTS operation, which is an advantage over the case of using a lumped chip inductor. The SAR study also indicates that the proposed antenna can meet the SAR limit for placing at the bottom of the mobile phone in practical applications.

REFERENCES

1. T.W. Kang and K.L. Wong, Chip-inductor-embedded small-size printed strip monopole for WWAN operation in the mobile phone, Microwave Opt Technol Lett 51 (2009), 966–971.
2. K.L. Wong, G.Y. Lee, and T.W. Chiou, A low-profile planar monopole antenna for multiband operation of mobile handsets, IEEE Trans Antennas Propag 51 (2003), 121–125.
3. K.L. Wong, Y.C. Lin, and T.C. Tseng, Thin internal GSM/DCS patch antenna for a portable mobile terminal, IEEE Trans Antennas Propag 54 (2006), 238–242.
4. K.L. Wong, Y.C. Lin, and B. Chen, Internal patch antenna with a thin air-layer substrate for GSM/DCS operation in a PDA phone, IEEE Trans Antennas Propag 55 (2007), 1165–1172.
5. Y.W. Chi and K.L. Wong, Internal compact dual-band printed loop antenna for mobile phone application, IEEE Trans Antennas Propag 55 (2007), 1457–1462.
6. W.Y. Li and K.L. Wong, Internal printed loop-type mobile phone antenna for penta-band operation, Microwave Opt Technol Lett 49 (2007), 2595–2599.
7. C.I. Lin and K.L. Wong, Printed monopole slot antenna for internal multiband mobile phone antenna, IEEE Trans Antennas Propag 55 (2007), 3690–3697.
8. C.H. Wu and K.L. Wong, Hexa-band internal printed slot antenna for mobile phone application, Microwave Opt Technol Lett 50 (2008), 35–38.
9. K.L. Wong and T.W. Kang, GSM850/900/1800/1900/UMTS printed monopole antenna for mobile phone application, Microwave Opt Technol Lett 50 (2008), 3192–3198.
10. Y.W. Chi and K.L. Wong, Very-small-size printed loop antenna for GSM/DCS/PCS/UMTS operation in the mobile phone, Microwave Opt Technol Lett 51 (2009), 184–192.
11. H. Wang, M. Zheng, and S.Q. Zhang, Monopole slot antenna, U.S. Patent 6,618,020 B2, September 9, 2003.
12. A.P. Zhao and J. Rahola, Quarter-wavelength wideband slot antenna for 3–5 GHz mobile applications, IEEE Antennas Wireless Propag Lett 4 (2005), 421–424.
13. P. Lindberg, E. Ojefors, and A. Rydberg, Wideband slot antenna for low-profile hand-held terminal applications, In Proceedings of the 36th European Microwave Conference (EuMC2006), Manchester, UK, 2006, pp. 1698–1701.
14. K.L. Wong and S.J. Liao, Uniplanar coupled-fed printed PIFA for WWAN operation in the laptop computer, Microwave Opt Technol Lett 51 (2009), 549–554.
15. K.L. Wong and F.H. Chu, Internal planar WWAN laptop computer antenna using monopole slot elements, Microwave Opt Technol Lett 51 (2009), 1274–1279.
16. T.H. Chang and J.F. Kiang, Meshed antenna reduction by embedding inductors, In IEEE AP-S International Symposium and USNC/

URSI National Radio Science Meeting, Session 78, Washington, DC, USA, 2005.
17. J. Thaysen and K.B. Jakobsen, A size reduction technique for mobile phone PIFA antennas using lumped inductors, Microwave J 48 (2005), 114–126.
18. S. Gevorgyan, O. Aval, B. Hansson, H. Jacobsson, and T. Lewin, Loss considerations for lumped inductors in silicon MMICs, In: IEEE MTT-S International Microwave Symposium, vol. 3, Anaheim, CA, USA, 1999, pp. 859–862.
19. J.C. Lin, Specific absorption rates induced in head tissues by microwave radiation from cell phones, Microwave 2 (2001), 22–25.
20. Y.W. Chi and K.L. Wong, Compact multiband folded loop chip antenna for small-size mobile phone, IEEE Trans Antennas Propag 56 (2008), 3797–3803.
21. M.R. Hsu and K.L. Wong, Seven-band folded-loop chip antenna for WWAN/WLAN/WiMAX operation in the mobile phone, Microwave Opt Technol Lett 51 (2009), 543–549.
22. C.T. Lee and K.L. Wong, Uniplanar coupled-fed printed PIFA for WWAN/WLAN operation in the mobile phone, Microwave Opt Technol Lett 51 (2009), 1250–1257.
23. Ansoft Corporation HFSS, Available at: http://www.ansoft.com/products/hf/hfss/.
24. K.L. Wong, Planar antennas for wireless communications, Wiley, New York, 2003.
25. Schmid & Partner Engineering AG (SPEAG), SEMCAD, Available at: http://www.semcad.com.

A NOVEL CSRR-BASED DEFECTED GROUND STRUCTURE WITH DUAL-BANDGAP CHARACTERISTICS

Shu-Hong Fu,[1,2] and Chuang-Ming Tong[1,2]
[1] Department of Radar Engineering, Missile Institute of Air Force Engineering University, Sanyuan, Shaanxi 713800, China; Corresponding author: fushuhong1982@163.com
[2] State Key Laboratory of Millimeter Wave, Nanjing 210096, China

Received 16 March 2009

ABSTRACT: *A new type of dumbbell-shaped defected ground structure (DGS) is introduced in this article. Its dual-bandgap characteristics are reported for the first time and can be adjusted by changing the dimension of complementary split-ring resonators (CSRR) unit and gap. The dual bandstop filter using proposed DGS is designed and fabricated. Measured results show that there are two bandgaps centered at 3.35 GHz and 5.82 GHz, respectively.* © 2009 Wiley Periodicals, Inc.
Microwave Opt Technol Lett 51: 2908–2910, 2009; Published online in Wiley InterScience (www.interscience.wiley.com).
DOI 10.1002/mop.24776

Key words: *defected ground structure (DGS); complementary split-ring resonators (CSRR); dual-bandgap*

1. INTRODUCTION

Since defected ground structure (DGS) was proposed by Park et al. in 1999 [1], numerous researches have been done to propose many defected patterns boasting excellent bandgap characteristics [2–9], among them, dumbbell-shaped DGS occupied a lot, which is composed of rectangle and gap parts. In the literature, we have consulted so far, dumbbell-shaped DGS can be divided into two types according to defected patterns. One type is based on the shape of rectangle part. The derivatives include circle-shaped DGS [2], semicircle-shaped DGS [3], cross-shaped DGS [4], arrow-head DGS [5], spiral DGS [6, 7], and so on.

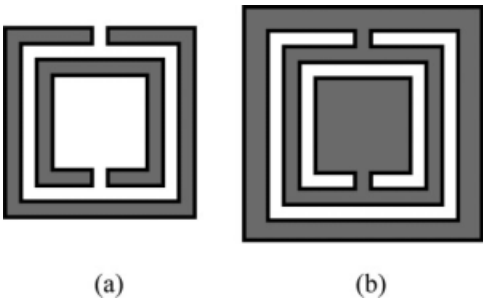

Figure 1 The geometries of split ring (SRR) and complementary split ring resonator (CSRR) (a) SRR (gray region is metal, white region is substrate) (b) CSRR (gray region is metal, white region is substrate)

The other type is based on the shape of gap part. This type is typically represented by interdigital DGS [10, 11].

The split-ring resonator (SRR), originally proposed by Pendry et al. [12], have attracted a great deal of interest for the design of negative permeability and left-handed (LH) effective media [13]. The complementary split-ring resonator (CSRR) [14–16] is the negative image of the SRR, which can provide a negative effective permittivity in the vicinity of its resonant frequency and produces sharp rejection band.

In this article, a new type of dumbbell-shaped DGS is presented, which adopts the CSRR, instead of the conventional rectangle part, called CSRR-based DGS. When compared with conventional structure, the new structure has remarkable dual-bandgap characteristics, which can be controlled by adjusting the dimension of CSRR and direct gap. A dual bandstop filter using CSRR-based DGS was designed and fabricated. Measurement and simulation results are in a good agreement.

2. DESIGN OF CSRR-BASED DEFECTED GROUND STRUCTURE

Figure 1(a) illustrates the geometry of one CSRRs, which is the negative image of the SRR shown in Figure 1(b). The CSRR-based DGS is implemented incorporating CSRRs and direct joint gap, as shown in Figure 2. In this figure, the gray region is the microstrip line and the grayish region is ground plane, where DGS is etched. In the conventional dumbbell-shaped DGS, the rectangle part is square configuration.

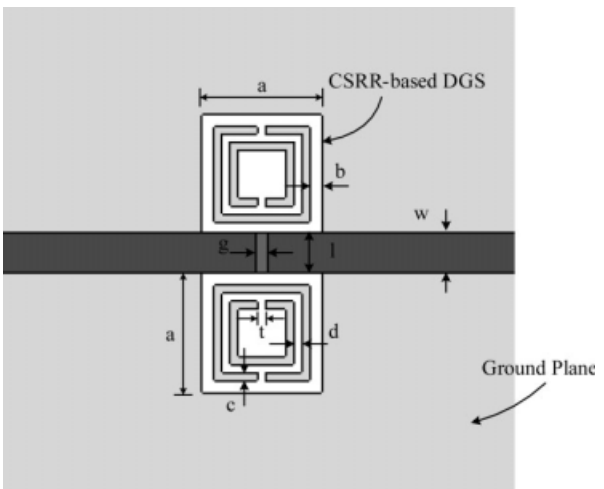

Figure 2 The proposed CSRR-based DGS